混合能源供应的绿色蜂窝网络智能能源与交通协调

Intelligent Energy and Traffic Coordination for Green Cellular Networks With Hybrid Energy Supply

Min Sheng, *Senior Member, IEEE*, Daosen Zhai, Xijun Wang, *Member, IEEE*, Yuzhou Li, Yan Shi, *Member, IEEE*, and Jiandong Li, *Senior Member, IEEE*

***Abstract*—In energy-harvesting-enabled networks, the intermittent and randomly distributed renewable energy imposes severe challenges in reliably supplying the time-varying mobile traffic. To tackle this issue, we reshape the spatial renewable energy and mobile traffic by exploiting the approach of energy sharing and load shifting, with the objective of minimizing the grid energy expenditure of cellular networks powered by both grid and renewable energy. We formulate this problem as a mixed-integer nonlinear programming, which is proved to be NP-hard. For centralized networks, we first devise a cost-efficient centralized algorithm leveraging the univariate search technique, which can find the near-optimal solutions with the advantages of low complexity and fast convergence. Specifically, by jointly optimizing the spatial distribution of renewable energy and mobile traffic, the centralized algorithm achieves a good match between the renewable energy supply and the total energy demand at each base station (BS), such that the grid energy expenditure of the whole network is greatly reduced. For distributed networks, we further propose a three-phase distributed control policy in which BSs and mobile users adjust their strategies independently only with their local information. Finally, we present extensive simulations to investigate the convergence and effectiveness of our proposed algorithms and demonstrate the achieved energy conservation gain compared with the existing schemes.**

***Index Terms*—Energy cooperation, energy harvesting, green communication, load distribution, renewable energy.**

I. Introduction

THE explosive increase in mobile communication devices and ubiquitous wireless services has incurred significant energy consumption and carbon footprints. It has been estimated that 2%–10% of global energy consumption and about 2% of worldwide CO_2 emissions are caused by the information and communication technology industry, wherein base stations (BSs) contribute to 60%–80% of the total energy expenditure [1]–[3]. Moreover, this situation will be further aggravated with the evolution of fifth-generation mobile communications, as the forecast shows that the amount of data handled by wireless networks will have increased by well over a factor of 100 in just a decade from 2010 to 2020 [4]. Under the pressures from both ecology and economy, green communication has thereby become an inevitable trend for future wireless networks [5].

To cater for the vision of green communications, various energy-saving techniques, such as resource allocation [6], BS switching [7], cell zooming [8], etc., have been proposed in cellular networks. In addition to reducing the energy consumption on the demand side [6]–[8], powering communication systems with renewable energy on the supply side is another effective approach to reduce grid energy cost [5], [9]. As an ecological and economic friendly technique, energy harvesting, which can scavenge cheap and clean renewable energy from ambient environment, has attracted extensive attention and inspired thorough research in both academia [5], [9] and industry [10]–[12]. For instance, Huawei [10] has designed solar-energy-powered cellular BSs in Bangladesh. Ericsson [11] and Nokia Siemens Networks [12] have also developed green BSs with energy supplied by solar panels and wind turbines to avoid using any grid electricity.

Nevertheless, unlike reliable grid energy provided by power plants, renewable energy is highly dependent on weather and location, resulting in its intermittence and randomness. Hence, the conventional energy-saving techniques can hardly be applied to the green cellular networks equipped with energy harvesting devices; thus, dedicated energy management schemes should be designed for them. If the renewable energy profile is deterministic or known ahead of time, the offline energy management schemes can be devised to utilize the intermittently available renewable energy optimally [13]–[15]. However, in practice, exact information on the time-varying energy harvesting process is hard to acquire. Therefore, how to deal with the time-varying behavior of the energy harvesting process is a critical issue.

As a potential solution, the geographical diversity of renewable energy can be utilized to mitigate the fluctuations of the energy harvesting process in time domains. To exploit the geographical energy diversity, research studies fall into two major categories, namely, energy-aware load shifting [16]–[18] and load-oriented energy cooperation [19]–[22]. For the first category, Zhou *et al.* in [16] adopted user association and power control to reduce the grid energy consumption in hybrid-energy-powered cellular networks. With the same objective, intelligent cell breathing was introduced in [17] to associate more users to the BSs with a large energy harvesting rate.

Manuscript received August 12, 2015; revised February 26, 2016; accepted April 9, 2016. Date of publication April 15, 2016; date of current version February 10, 2017. This work was supported in part by the National Natural Science Foundation of China under Grant 61231008 and Grant 61301176; by the 111 Project under Grant B08038; and by the 863 Project under Grant 2014AA01A701. The review of this paper was coordinated by Prof. A. Jamalipour.

M. Sheng, D. Zhai, X. Wang, Y. Shi, and J. Li are with the State Key Laboratory of Integrated Service Networks, Xidian University, Xi'an 710071, China (e-mail: msheng@mail.xidian.edu.cn; jdli@mail.xidian.edu.cn; zhaidaosen@stu.xidian.edu.cn; xijunwang@xidian.edu.cn; yshi@xidian.edu.cn).

Y. Li is with the School of Electronic Information and Communications, Huazhong University of Science and Technology, Wuhan 430074, China (e-mail: yuzhouli@hust.edu.cn).

Color versions of one or more of the figures in this paper are available online at http://ieeexplore.ieee.org.

Digital Object Identifier 10.1109/TVT.2016.2554618

0018-9545 © 2016 IEEE. Personal use is permitted, but republication/redistribution requires IEEE permission.
See http://www.ieee.org/publications_standards/publications/rights/index.html for more information.
Authorized licensed use limited to: Huazhong University of Science and Technology. Downloaded on July 19,2024 at 08:11:44 UTC from IEEE Xplore. Restrictions apply.

Similarly, by adjusting the strength of the pilot signals, the work in [18] tackled the multistage energy allocation problem and the multicell energy balancing problem. As one of the main common features, the studies in [16]–[18] coordinate BSs' traffic load to match their energy harvesting rates via load shifting. Regarding the load-oriented energy cooperation category, Chia *et al.* in [19] investigated the energy exchange strategies between two BSs through a direct power line. Under the smart grid framework, Guo *et al.* in [20] addressed the energy-saving issue by jointly considering energy and spectrum cooperation. In CoMP systems, the energy sharing and trading problems were investigated in [21] and [22], respectively. A more comprehensive study for joint energy and communication cooperation can be found in [23].

Although the existing works exploit the geographical energy diversity, renewable energy has not been fully utilized. This is because traffic load and renewable energy are not well matched. More specifically, for the studies in [16]–[18], the performance of these methods is limited, as load shifting can only be utilized for cell-edge users. As a consequence, some BSs with a light traffic load may still be sufficient in renewable energy, whereas others with a heavy traffic load may suffer from renewable energy deficits. Hence, renewable energy is not fully utilized only through coordinating the load distribution among BSs. On the other hand, the studies in [19]–[22] neglect the coordination in traffic load, which may result in a suboptimal configuration between renewable energy and traffic load. This is because in some cases, offloading mobile traffic to the underloaded BSs with abundant renewable energy can save more grid energy, as the energy exchange leads to additional energy cost. Moreover, an unbalanced load distribution leads to heavy burden on some BSs that have to use large transmission power to satisfy the rate requirements of all users, which, in turn, produces strong interference to the users located in the adjacent cells.

Motivated by the given analysis, in this paper, we formulate a novel energy and traffic matching problem by jointly considering energy sharing and load shifting. The incorporation of energy sharing and load shifting is a new energy and communication cooperation paradigm that can fully exploit the renewable energy and hence reduce conventional grid energy expenditure. The main contributions of this paper are as follows.

- We formulate the grid energy cost minimization problem as a mixed-integer nonlinear programming by jointly considering user association, resource allocation, power control, and energy cooperation. The NP-hardness of this problem is proved by equating it to a bin packing problem.
- For centralized networks, we borrow the idea of a univariate search technique to design a cost-efficient algorithm, which can achieve near-optimal solutions with the advantages of low complexity and fast convergence. In particular, the centralized algorithm optimizes the load distribution (i.e., user association and resource allocation) and energy configuration (i.e., power control and energy cooperation) iteratively, such that the objective value keeps decreasing until convergence.
- For distributed networks, we further propose a distributed control policy based on the design philosophy of the centralized algorithm. Specifically, the distributed control policy consists of three phases: load-aware user association, intracell power and resource allocation, and intercell energy cooperation, which are independently executed at mobile users (MUs) and BSs only with their local information.
- Finally, we provide extensive simulations to investigate the convergence and effectiveness of our proposed algorithms and demonstrate the achieved performance gain compared with the existing schemes in terms of grid power consumption, average transmission power, and wasted renewable energy.

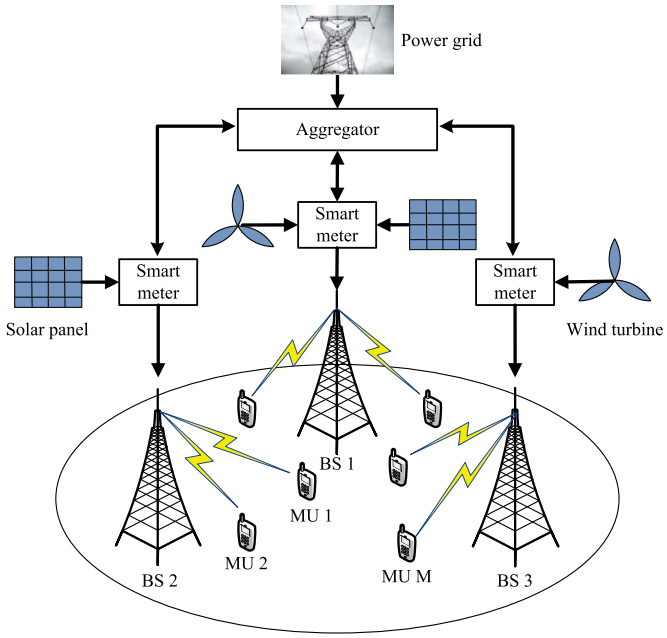

Fig. 1. Multicell cellular network with hybrid energy supply enhanced by energy cooperation.

The remainder of this paper is organized as follows. Section II introduces the concerned system model. In Section III, we present the problem formulation and theoretical analysis. The centralized and distributed algorithms are elaborated in Sections IV and V, respectively. Section VI shows the simulation results. Finally, we conclude our paper in Section VII.

II. System Model

Here, we introduce the concerned communication model and energy supply model.

A. Communication Model

As shown in Fig. 1, we consider the downlink network consisting of N BSs and M MUs, both of which are equipped with a single antenna. For notational simplicity, we denote the set of BSs and MUs by $\mathcal{B}$ and $\mathcal{U}$, respectively, i.e., $\mathcal{B} = \{1, 2, \ldots, N\}$ and $\mathcal{U} = \{1, 2, \ldots, M\}$. The total bandwidth of the system is W, which is shared among BSs (i.e., frequency reuse factor is 1) [24], [25]. Let $\mathbf{P} = (P_1^t, P_2^t, \ldots, P_N^t)$ denote the transmission

Authorized licensed use limited to: Huazhong University of Science and Technology. Downloaded on July 19,2024 at 08:11:44 UTC from IEEE Xplore. Restrictions apply.

power of all BSs, which can be adjusted to mitigate intercell interference. In addition, the channel power gain from BS n to MU m is defined as $g_{n,m}$, which accounts for the path loss and shadowing. Furthermore, we assume that the channel condition is static during the underlying operational period[1] and perfectly known at BSs.[2]

Each MU is located in the coverage area of one or multiple BSs. At any given time, each MU can be served by only one BS, but each BS can serve multiple MUs. To represent the relationship between BSs and MUs, we introduce a matrix $\mathbf{X} = (x_{n,m})$, where $x_{n,m} = 1$ if MU m is associated with BS n; otherwise, $x_{n,m} = 0$. For the MUs associated with the same BS, we assume that the communication resources (time slot, frequency band, or resource block) are shared among the MUs, as in [24] and [25]. Thus, our considered system is a general case that can be a network based on time-division multiple access, frequency-division multiple access, or orthogonal frequency-division multiple access. Furthermore, we denote the ratio of communication resource acquired by MU m from BS n as $y_{n,m}$ and set $\mathbf{y}_n = (y_{n,1}, y_{n,2}, \ldots, y_{n,M})$ and $\mathbf{Y} = (\mathbf{y}_1, \mathbf{y}_2, \ldots, \mathbf{y}_N)$.

If MU m is associated with BS n, its achievable data rate [24], [25] can be expressed as

$$R_{n,m} = y_{n,m} W \log_2 \left(1 + \frac{P_n^t g_{n,m}}{\sum\limits_{n' \in \mathcal{B}, n' \neq n} P_{n'}^t g_{n',m} + \eta}\right) = y_{n,m} \overline{R}_{n,m} \quad (1)$$

where η is the noise power, and $\overline{R}_{n,m}$ is the maximum instantaneous transmission rate from BS n to MU m.

B. Energy Supply Model

In our considered scenario, each BS n is capable of harvesting renewable energy from the environment through solar panels and/or wind turbines, the energy harvesting rate of which is denoted by E_n. Considering the practical factors of a short lifetime, limited capacity, and the high expense of existing batteries, we make the same assumptions as in [20] and [21] that the harvested energy cannot be stored for dynamic energy management. That is, the harvested energy is wasted if it is not utilized in time. Although the current wireless communication systems are usually equipped with batteries, they are generally used for backup in case of power supply outage instead of for dynamic energy management with frequent power charging and discharging. On the other hand, due to the fluctuation and unreliability of the energy harvesting process, conventional grid energy should also be provided as a supplement to guarantee reliable transmission.

[1]Without loss of generality, we normalize the operation period to a unit time so that the power and energy can mathematically add or subtract each other.

[2]If the channel state information cannot be acquired by BSs accurately, a robust problem formulation can be adopted. It is noted that our designed algorithms in this paper can also be applied to the robust problem only by considering the worst case channel condition and adjusting the parameters accordingly.

Next, we specify the energy cooperation among BSs, which can be implemented under the smart grid framework [26]. In a smart grid, the aggregator is a virtual entity that allows the BSs to either draw from or inject energy to it under different demand/supply conditions. Moreover, the whole process of energy harvesting, consumption, and drawing/injecting at each BS can be coordinated by a smart meter [20]–[23]. Let $\mathbf{E} = (e_{n,n'})$ denote the energy transfer among BSs, where $e_{n,n'}$ represents the energy transferred from BS n to BS n'. Due to the resistive loss of power line and the processing overhead, some energy will be consumed during the energy injection and extraction procedures inevitably. As such, BS n' can receive energy $\alpha_{n,n'} e_{n,n'}$ only from the aggregator, where $0 < \alpha_{n,n'} < 1$ denotes the loss factor from BS n to BS n' [19]. Practically, $\alpha_{n,n'}$ consists of two parts $\alpha_{n,a}$ and $\alpha_{n',a}$ that are the loss factors from BS n to the aggregator and from the aggregator to BS n', respectively. With energy cooperation, the available renewable energy of BS n becomes

$$\begin{aligned}\xi_n &= E_n + \sum_{n' \in \mathcal{B}, n' \neq n} \alpha_{n',n} e_{n',n} - \sum_{n' \in \mathcal{B}, n' \neq n} e_{n,n'} \\ &= E_n + \sum_{n' \in \mathcal{B}, n' \neq n} (\alpha_{n',n} e_{n',n} - e_{n,n'}). \end{aligned} \quad (2)$$

It is worth pointing out that $e_{n',n}$ and $e_{n,n'}$ cannot be larger than zero simultaneously in a practical system, as the bidirectional energy exchange leads to additional energy cost.

III. Problem Formulation and Analysis

Here, we begin with formulating the grid energy conservation problem, followed by analyzing its properties.

A. Problem Formulation

We investigate the grid energy conservation problem by jointly considering power control $\mathbf{P}$, user association $\mathbf{X}$, resource allocation $\mathbf{Y}$, and energy cooperation $\mathbf{E}$, which is formulated as

$$\begin{aligned} \min_{\mathbf{P},\mathbf{X},\mathbf{Y},\mathbf{E}} \; & P_G^{\text{tot}} = \sum_{n \in \mathcal{B}} \left(\rho_n P_n^t + P_n^c - \xi_n\right)^+ \\ \text{s.t.C1} : & \sum_{n \in \mathcal{B}} y_{n,m} \overline{R}_{n,m} \geq R_m^{\text{req}} \, \forall \, m \\ \text{C2} : & \sum_{m \in \mathcal{U}} y_{n,m} \leq 1 \, \forall \, n \\ \text{C3} : & \sum_{n \in \mathcal{B}} x_{n,m} = 1 \, \forall \, m \\ \text{C4} : & \, 0 \leq y_{n,m} \leq x_{n,m}, \; x_{n,m} \in \{0,1\} \, \forall \, n, m \\ \text{C5} : & \, \xi_n = E_n + \sum_{n' \in \mathcal{B}, n' \neq n} (\alpha_{n',n} e_{n',n} - e_{n,n'}) \, \forall \, n \\ \text{C6} : & \, 0 \leq P_n^t \leq P_n^{\max} \, \forall \, n \end{aligned} \quad (3)$$

Authorized licensed use limited to: Huazhong University of Science and Technology. Downloaded on July 19,2024 at 08:11:44 UTC from IEEE Xplore. Restrictions apply.

where $(x)^+ = \max\{x, 0\}$, $\rho_n \geq 1$ denotes the inefficiency of the power amplifier, and P_n^c represents the static power consumption of BS n caused by baseband processing and cooling.

In (3), we aim to minimize the total grid energy consumption P_G^{tot} subject to C1–C6. C1 specifies the minimum rate requirement of each MU. C2 ensures that the total percentage of allocated resource at each BS is no larger than 1. C3 indicates that each MU can be associated with only one BS. C4 guarantees that each BS can only serve the MUs associated with it. C6 is the maximum transmission power constraint, which is imposed by the hardware limitation or standard regulation.

Remark 1: Problem (3) is a unified study on smart grid, cellular network, and energy harvesting, which can provide engineering guidelines for the design of green communication systems. The joint optimization of energy sharing and load shifting is a new energy and communication cooperation paradigm that helps us fully exploit the geographical diversity of renewable energy. Our study caters to the green evolution of the current power and communication systems.

Remark 2: 1) It is noteworthy that (3) may become infeasible particularly in case of overload. To deal with this case, it is necessary to formulate the admission control into the model, which is beyond the scope of this paper. 2) Throughout this paper, we assume that (3) is always feasible, such as by the conventional best signal-to-interference-plus-noise ratio method (Best SINR).[3]

B. Theoretical Analysis

To tackle the nonsmoothness of the objective function in (3), we present the following lemma to reformulate it as a smooth objective function.

Lemma 1: Problem (3) can be equivalently recast as

$$\min_{\mathbf{P},\mathbf{X},\mathbf{Y},\mathbf{E}} \; P_G^{\text{tot}} = \sum_{n\in\mathcal{B}} \left(\rho_n P_n^t + P_n^c - \xi_n\right)$$
$$\text{s.t. C1, C2, C3, C4, C5}$$
$$\text{C6}' : \frac{\xi_n - P_n^c}{\rho_n} \leq P_n^t \leq P_n^{\max} \; \forall n. \tag{4}$$

Proof: For (3), two conditions should be considered: 1) The renewable energy is insufficient to meet the total energy demand; and 2) the renewable energy is sufficient to meet the total energy demand. In what follows, we discuss these two conditions, respectively.

1) The renewable energy is insufficient: In this case, the system will consume grid energy, i.e., $P_G^{\text{tot}} > 0$. Accordingly, the optimal control policy must satisfy $\rho_n P_n^t + P_n^c \geq \xi_n \; \forall n$, which can be proved by contradiction. Assume there exists a BS n with $\rho_n P_n^t + P_n^c < \xi_n$ for the optimal control policy $\mathcal{P}$. Then, this BS can transfer its surplus renewable energy $\xi_n - \rho_n P_n^t - P_n^c$ to other BSs with $\rho_{n'} P_{n'}^t + P_{n'}^c > \xi_{n'}$. As a result, the total grid energy consumption can be further reduced, which violates the optimality of the control policy $\mathcal{P}$. Thus, the condition $\rho_n P_n^t + P_n^c \geq \xi_n \; \forall n$ must hold for the optimal control policy, and (3) can be equivalently recast as (4) in this case.
2) The renewable energy is sufficient: In this case, the total grid energy consumption becomes zero, i.e., $P_G^{\text{tot}} = 0$, and (3) degrades into the following problem:

$$\text{find}: \; \left\{\mathbf{P}, \mathbf{X}, \mathbf{Y}, \mathbf{E} | \text{C1}, \text{C2}, \text{C3}, \text{C4}, \text{C5}, P_G^{\text{tot}} = 0\right\}. \tag{5}$$

For the given problem, the feasible solution is usually not unique, from which we can always find one satisfying $\rho_n P_n^t + P_n^c = \xi_n \; \forall n$ and C1–C5. In a practical system, this solution can be acquired through improving the transmission power of all or partial BSs to run out of the redundant renewable energy. Furthermore, it is noted that this solution can also be acquired by directly solving (4), as (4) includes the solution with $\rho_n P_n^t + P_n^c = \xi_n \; \forall n$.

To this end, we complete the proof of Lemma 1. ■

Remark 3: It is difficult to judge which condition of (3) holds (i.e., the renewable energy is sufficient to support the whole system or its opposite case). Lemma 1 unifies these two conditions, which will help us simplify the algorithm design.

Theorem 1: The grid energy conservation problem (4) is NP-hard.

Proof: There are four groups of optimization variables to be optimized for (4), which are mutually coupled and jointly determine the objective value. To reveal the nature of (4) more clearly, we make some simplifying assumptions. First, we assume that the optimal energy configuration scheme $\{\mathbf{P}^*, \mathbf{E}^*\}$ has been acquired in advance, then (4) is transformed into the following load distribution problem (LDP), i.e., finding a feasible user association and resource allocation policy to meet all MUs' rate requirement:

$$\text{find } \{\mathbf{X}, \mathbf{Y} | \text{C1}, \text{C2}, \text{C3}, \text{C4}\}. \tag{6}$$

For (6), we further assume that the resource is allocated by each BS to exactly satisfy the minimum rate requirement of all MUs associated with it, i.e., $y_{n,m} = R_m^{\text{req}}/\overline{R}_{n,m}$ if MU m is associated with BS n. To this end, (6) can be expressed as the following question.

Question: Is there a partition of $\mathcal{U} = \{1, 2, \ldots, M\}$ into N disjoint sets $U_1, U_2, \ldots, U_N$ such that the sum of the sizes of the items in each U_n is less than or equal to 1? Specifically, the size of each item in U_n is a deterministic value as $y_{n,m} = R_m^{\text{req}}/\overline{R}_{n,m}$.

The given question is a typical bin packing problem, which is NP-hard [27]. Since a bin packing problem is always embedded in (4), this problem is NP-hard as well. ■

In addition to the NP-hardness, (4) is also a nonconvex programming due to the nonconvex constraint C1, which means that (4) might have multiple local optima. What is worse is that the coupling property between user association $\mathbf{X}$ and other optimization variables $\{\mathbf{P}, \mathbf{Y}, \mathbf{E}\}$ makes (4) more intractable. In view of these, this paper is devoted to designing cost-efficient algorithms.

[3]The Best SINR method always associates an MU to the BS with the strongest received signal, e.g., pilot signal.

Authorized licensed use limited to: Huazhong University of Science and Technology. Downloaded on July 19,2024 at 08:11:44 UTC from IEEE Xplore. Restrictions apply.

IV. Description of the Centralized Algorithm

Here, we propose a centralized algorithm to tackle (4) based on the univariate search technique in optimization theory. The centralized algorithm is suitable for the network with a central controller that can aggregate all distributed information, as the emerging cloud radio access network. Moreover, the centralized algorithm enables us to obtain the performance upper bound and characterize the theoretical limits of practical systems.

A. Joint Energy Sharing and Load Shifting

The general algorithm procedure, which is summarized in Algorithm 1, is detailed in the following. We initialize the transmission power of each BS as their maximum values and set the total grid energy consumption as $P_G(0) = \sum_{n\in\mathcal{B}}(\rho_n P_n^{\max} + P_n^c - E_n)^+$. Furthermore, we define an indicator variable ς to denote whether the renewable energy is sufficient to support the whole system ($\varsigma = 1$) or not ($\varsigma = 0$). After the initialization, the joint energy sharing and load shifting algorithm (JESLS) solves the LDP and the energy configuration problem (ECP) alternately until satisfying the end conditions. In detail, when the transmission power and energy cooperation are fixed, the JESLS optimizes the load distribution among BSs with the objective of maximizing each MU's transmission rate, which is beneficial for bringing down the total grid energy consumption in the next operation. Then, given the user association and resource allocation, the JESLS minimizes the total grid energy consumption by performing power control and energy cooperation correspondingly.

Algorithm 1 JESLS

1: **Initialization**: Set $t=0$, the energy sufficient indicator $\varsigma = 0$, and the maximum tolerance $\varepsilon_1 > 0$. Set $\mathbf{P}(0) = (P_1^{\max}, \ldots, P_n^{\max})$ and $P_G(0) = \sum_{n\in\mathcal{B}}(\rho_n P_n^{\max} + P_n^c - E_n)^+$;
2: **repeat**
3: $t = t + 1$;
4: Obtain $\{\mathbf{X}(t), \mathbf{Y}(t)\}$ for given $\{\mathbf{P}(t-1), \mathbf{E}(t-1)\}$ by solving the LDP (7);
5: Obtain $\{\mathbf{P}(t), \mathbf{E}(t)\}$ for given $\{\mathbf{X}(t), \mathbf{Y}(t)\}$ by solving the ECP (11);
6: Calculate $P_G(t) = \sum_{n\in\mathcal{B}}(\rho_n P_n^t(t) + P_n^c - \xi_n(t))^+$;
7: **until** $\varsigma = 1$ or $|P_G(t-1) - P_G(t)| < \varepsilon_1$

B. Load Distribution Problem

By fully exploiting the service capability of each BS, the transmission rates of all MUs can be greatly improved [24]. If the transmission rates of all MUs are larger than their own demands, the transmission power of BSs can be degraded, and hence the total grid energy consumption can be further decreased. Furthermore, the minimum transmission power of a BS is usually limited by the MU with the minimum redundant transmission rate, which is similar to the cask effect. Based on these guidelines, we formulate the LDP as the following max-min redundant rate problem:

$$\max_{\mathbf{X},\mathbf{Y}} \min_{m\in\mathcal{U}} \sum_{n\in\mathcal{B}} y_{n,m}\overline{R}_{n,m} - R_m^{\text{req}} \quad \text{s.t. C1, C2, C3, C4.} \tag{7}$$

To tackle the nonsmoothness of the objective function in (7), we introduce a new variable φ to transform the original problem (7) into its epigraph form, i.e.,

$$\max_{\mathbf{X},\mathbf{Y},\varphi\geq 0} \varphi \quad \text{s.t. C1}' : \sum_{n\in\mathcal{B}} y_{n,m}\overline{R}_{n,m} \geq R_m^{\text{req}} + \varphi \,\forall\, m \quad \text{C2, C3, C4.} \tag{8}$$

Theorem 2: The max-min redundant rate problem (8) is NP-hard.

Proof: Similar with (4), (8) is also embedded with a bin packing problem, resulting in its NP-hardness. ■

The NP-hardness indicates that we cannot find a polynomial-time algorithm to obtain the global optimum of (8). Although Bender's decomposition [28] and branch-and-bound [29] methods can solve it optimally, they consume abundant computational time and cannot be applied for large-scale networks. Despite these, a suboptimal solution with $\varphi > 0$ is still useful for reducing the total grid energy consumption in the energy configuration phase. Furthermore, it is worth noting that the optimum of (8) is just the intermediate result for (4) and may not necessarily be the final optimal solution. Based on these, we concentrate on devising an effective algorithm to seek the solutions with $\varphi > 0$ (or called feasible solution).

To eliminate the coupling between $\mathbf{X}$ and $\mathbf{Y}$, we first relax each $x_{n,m}$ to a continuous interval, i.e., $x_{n,m} \in [0, 1]$. In this context, $x_{n,m}$ can denote both user association and resource allocation, since $x_{n,m} > 0$ indicates that MU m is associated with BS n, whereas $x_{n,m} = 0$ indicates no association, and, furthermore, its value specifies the fraction of resource acquired by MU m from BS n. Therefore, the resource allocation variables $\mathbf{Y}$ can be replaced by $\mathbf{X}$ after the relaxation, and accordingly, the relaxed problem is formulated as

$$\begin{aligned} &\max_{\mathbf{X},\varphi\geq 0} \varphi \\ &\text{s.t. C1}'' : \sum_{n\in\mathcal{B}} x_{n,m}\overline{R}_{n,m} \geq R_m^{\text{req}} + \varphi \,\forall\, m \\ &\quad \text{C2}' : \sum_{m\in\mathcal{U}} x_{n,m} \leq 1 \,\forall\, n \\ &\quad \text{C4}' : 0 \leq x_{n,m} \leq 1 \,\forall\, n, m \\ &\quad \text{C7} : x_{n,m} = 0, \text{if } m \in \mathcal{BL}_n \,\forall\, n, m \end{aligned} \tag{9}$$

where C7 is a newly imposed constraint to guarantee the convergence of Algorithm 2, which will be further discussed in the latter part. Compared with the original mixed-integer linear programming (8), (9) becomes much more easier to tackle, since it is just linear programming (LP) with less optimization variables.

To get a feasible solution of (8) effectively, a polynomial-time algorithm, namely, linear programming deflation algorithm

Authorized licensed use limited to: Huazhong University of Science and Technology. Downloaded on July 19,2024 at 08:11:44 UTC from IEEE Xplore. Restrictions apply.

(LPD), is proposed and summarized in Algorithm 2. The design philosophy of the LPD is to iteratively solve the relaxed LP (9) with a continuously contractive feasible region until getting a feasible solution of (8). Specifically, the LPD first finds a candidate solution by relaxation and rounding in each iteration, which corresponds to steps 3–6 in Algorithm 2. Then, each BS n detects whether it is capable of serving the MUs associated with it, i.e., the operations in steps 7–13. If all BSs pass the tests, a feasible solution is found, and the loop is terminated; otherwise, the feasible region will be shrunk to exclude the infeasible solutions. In particular, if BS n fails the detection, it will find the newly admitted user set, i.e., $\mathcal{NU}_n = \{m \mid x_{n,m} = 1 \text{ and } x'_{n,m} = 0\}$, where $\mathbf{X}'$ represents the previous user association scheme.[4] Then, BS n selects the MU that occupies the most resource from $\mathcal{NU}_n$ and adds it into its blacklist, which records the MUs prohibited to be associated with it. Note that the previous feasible user association scheme $\mathbf{X}'$ is still preserved after each deflation, and hence a feasible solution of (8) can be always obtained after finite iterations (the worse case is $\mathbf{X}'$). Finally, each BS allocates its resource to the MUs associated with it according to (10), shown at the bottom of the next page, which maximizes the minimum redundant rate of these MUs.

Algorithm 2 LPD

1: **Initialization**: Set the blacklist of each BS as an empty set, i.e., $\mathcal{BL}_n \Leftarrow \varnothing,\ \forall n$. Set the feasibility indicator $\omega = 1$. Set $\mathbf{X}'$ as the previous user association scheme.
2: **while** 1 **do**
3: Obtain $\mathbf{X}$ by solving the relaxed LP (9);
4: **for** each MU $m \in \mathcal{U}$ **do**
5: Find $n^* = \arg\max_{n\in\mathcal{B}} x_{n,m}\overline{R}_{n,m}$, and set $x_{n^*,m} = 1$ and $x_{n',m} = 0, \forall\, n' \neq n^*$;
6: **end for**
7: **for** each BS $n \in \mathcal{B}$ **do**
8: **if** $\sum_{m\in\mathcal{U}}(x_{n,m}R_m^{\text{req}}/\overline{R}_{n,m}) > 1$ **then**
9: Set $\omega = 0$;
10: Find the newly admitted user set, i.e., $\mathcal{NU}_n = \{m \mid x_{n,m} = 1 \text{ and } x'_{n,m} = 0\}$;
11: Find $m^* = \arg\max_{m\in\mathcal{NU}_n}(x_{n,m}R_m^{\text{req}}/\overline{R}_{n,m})$, and add MU m^* into the blacklist of BS n, i.e., $\mathcal{BL}_n \Leftarrow \mathcal{BL}_n \cup \{m^*\}$;
12: **end if**
13: **end for**
14: **if** $\omega = 1$ **then**
15: break;
16: **else**
17: Set $\omega = 1$;
18: **end if**
19: **end while**
20: Compute the resource allocation $\mathbf{Y}$ according to (10).

[4]It is noted that $\mathbf{X}'$ is always a feasible user association scheme for the given energy configuration policy $\{\mathbf{P}, \mathbf{E}\}$, as constraint C1 is satisfied when addressing the ECP (11) in the previous iteration. Moreover, on the first execution for the LPD, $\mathbf{X}'$ is set to the Best SINR method.

C. Energy Configuration Problem

Given user association and resource allocation, the remainder optimization problem of (4) is reformulated as

$$\min_{\mathbf{P},\mathbf{E}} \sum_{n\in\mathcal{B}} \left(\rho_n P_n^t + P_n^c - \xi_n\right) \quad \text{s.t. C1, C5, C6}'. \tag{11}$$

It is noted that (11) can be recast as an LP by appropriately rearranging C1 and solved by the existing algorithms, as the cutting-plane method [30]. However, solving the LP directly consumes abundant computational time, as (11) contains $N^2 + N$ optimization variables, and its asymptotic complexity is $O((N^2+N)^{3.5})$ [31]. To reduce computational complexity, we exploit the special structure of (11) to decompose it into two sequential subproblems and then solve them effectively.

Lemma 2: The optimal solution of (11) can be obtained by solving the following two subproblems sequentially.

1) Power control problem:

$$\min_{\mathbf{P}} \sum_{n\in\mathcal{B}} \rho_n P_n^t \quad \text{s.t. C1, C6.} \tag{12}$$

2) Energy cooperation problem:

$$\max_{\mathbf{E}} \sum_{n\in\mathcal{B}} \xi_n \quad \text{s.t. C5, C6}'. \tag{13}$$

Proof: See Appendix A. ■

To tackle (12) effectively, we design a simple iterative power control algorithm (IPC) based on the standard interference function [32], which is summarized in Algorithm 3. Primarily, we define the following equation:

$$f_{n,m}(\mathbf{P}) = \begin{cases} \frac{I_{n,m}(\mathbf{P})}{g_{n,m}}\left(2^{\frac{R_m^{\text{req}}}{Wy_{n,m}}} - 1\right), & \text{if } x_{n,m} = 1 \\ 0, & \text{if } x_{n,m} = 0 \end{cases} \tag{14}$$

where $I_{n,m}(\mathbf{P}) = \sum_{n'\in\mathcal{B},n'\neq n} P_{n'}^t g_{n',m} + \eta_m$.

Note that (14) represents the minimum transmission power needed by BS n to satisfy the rate requirement of MU m in the context that other BSs' transmission power values are fixed. Then, we define

$$T_n(\mathbf{P}) = \max_{m\in\mathcal{U}} f_{n,m}(\mathbf{P}). \tag{15}$$

Theorem 3: $T_n(\mathbf{P})$ is a standard interference function.

Proof: See Appendix B. ■

Remark 4: According to the standard interference function [32], [33], the IPC converges geometrically fast to the global optimum of (12) with any initial points. Moreover, as shown in Algorithm 3, the IPC only contains simple iterative operations without any complex calculations; thus, it is a computationally effective algorithm.

Authorized licensed use limited to: Huazhong University of Science and Technology. Downloaded on July 19,2024 at 08:11:44 UTC from IEEE Xplore. Restrictions apply.

Algorithm 3 IPC

1: **Initialization**: Set $k=0$ and the maximum tolerance $\varepsilon_2>0$. Set $\mathbf{P}(k)=\mathbf{P}(t)$ and $P_G(k)=\sum_{n\in\mathcal{B}}\rho_n P_n^t(k)$;
2: **repeat**
3: Calculate $I_{n,m}(\mathbf{P}(k))$ for all n and m;
4: Each BS n updates its transmission power according to $P_n^t(k+1)=T_n(\mathbf{P}(k))$;
5: Calculate $P_G(k+1)=\sum_{n\in\mathcal{B}}\rho_n P_n^t(k+1)$;
6: $k=k+1$;
7: **until** $|P_G(k)-P_G(k-1)|<\varepsilon_2$

After getting the optimal transmission power, we can to deal with (13), an LP. To further reduce the computational complexity, we exploit the structure property of the system, i.e., two-hop energy transfer framework, to design a simple algorithm, namely, sequential waterfilling algorithm (SWF), described in Algorithm 4. The design principle of the SWF comes from two points. The first point is that the BSs with sufficient renewable energy should transfer their redundant renewable energy to the aggregator, whereas others need to apply for renewable energy from the aggregator. The other point is that assigning the collected renewable energy in the aggregator to the BSs with small loss factors preferentially can reduce the unnecessary energy cost in the energy transfer procedures, which is more beneficial for reducing the total grid energy consumption. Based on these two points, we propose the SWF to tackle (13) instead of solving the LP directly.

Algorithm 4 SWF

All BSs are divided into two groups: renewable-energy-sufficient BSs, i.e., $\mathcal{B}_1=\{n|\rho_n P_n^t+P_n^c<E_n\}$, and renewable-energy-insufficient BSs, i.e., $\mathcal{B}_2=\{n|\rho_n P_n^t+P_n^c>E_n\}$;
All BSs in $\mathcal{B}_1$ transfer their redundant renewable energy to the aggregator, and thus, the total collected renewable energy is $E_C=\sum_{n\in\mathcal{B}_1}\alpha_{n,a}(E_n-\rho_n P_n^t-P_n^c)$;
Sort all BSs in $\mathcal{B}_2$ in order of nonascending loss factor from the aggregator to the BSs;
for each BS $n\in\mathcal{B}_2$ in the order **do**
  if $\alpha_{a,n}E_C\geq\rho_n P_n^t+P_n^c-E_n$ **then**
    The aggregator transfer energy $(\rho_n P_n^t+P_n^c-E_n)/\alpha_{a,n}$ to BS n;
    Set $E_C=E_C-((\rho_n P_n^t+P_n^c-E_n)/\alpha_{a,n})$;
  else
    The aggregator transfer energy E_C to BS n;
    Set $E_C=0$;
    break;
  end if
end for
if $E_C\geq 0$ **then**
  Set $\varsigma=1$;
end if

Remark 5: In addition to the advantages of reducing computational complexity, both the IPC and SWF are easier to implement in a distributed manner because the IPC only needs each BS to detect the strength of interference plus noise [i.e., $I_{n,m}(\mathbf{P})$] received by the MUs associated with it, and the SWF executes energy exchange only between the BSs and the aggregator but without any information interaction among BSs.

D. Computational Complexity Analysis

The JESLS contains two categories of operations: load distribution and energy configuration. Compared with the load distribution, the complexity of the energy configuration is extraordinarily low so that it can be neglected. For the load distribution, the computational complexity is mainly dominated by solving the LP (9), the asymptotic complexity of which is $O(N^{3.5}M^{3.5})$ [31]. Then, we consider the worst case that the rate requirement of each MU can be satisfied by only one BS and that each MU is restricted to the right BS only after $N-1$ deflations for the feasible region of (8). Thus, the LPD takes up to $(N-1)M+1$ iterations to find a feasible solution of (8). Denoting L as the expected number of iterations for a given error tolerance in the JESLS, we can obtain that the complexity of the centralized algorithm is

$$\begin{aligned} &O\left(L\left(((N-1)M+1)\,N^{3.5}M^{3.5}\right)\right)\\ &\quad=O\left(L(N^{4.5}M^{4.5}-N^{3.5}M^{4.5}+N^{3.5}M^{3.5})\right)\\ &\quad=O(LN^{4.5}M^{4.5}). \end{aligned} \tag{16}$$

In practice, an MU can only be associated with its adjacent BSs, and the number of neighboring BSs is usually much less than N. Therefore, the computational complexity of the centralized algorithm is actually much less than (16). Fig. 3 shows that the computational time of the JESLS is much less than that of the exhaustive search particularly for a large number of MUs.

V. Description of the Distributed Algorithm

Here, we propose a three-phrase distributed control policy based on the design philosophy of the centralized algorithm. The distributed control policy is suitable for the distributed and self-organized network as the existing heterogeneous network. Compared with the centralized algorithm, the distributed control policy can provide more engineering guidelines for practical communication protocols.

$$y_{n,m}=x_{n,m}\left(\frac{R_m^{\mathrm{req}}}{R_{n,m}}+\frac{\frac{1}{R_{n,m}}}{\sum_{m\in\mathcal{U}}\left(\frac{x_{n,m}}{R_{n,m}}\right)}\left(1-\sum_{m\in\mathcal{U}}\left(x_{n,m}\frac{R_m^{\mathrm{req}}}{R_{n,m}}\right)\right)\right) \tag{10}$$

Authorized licensed use limited to: Huazhong University of Science and Technology. Downloaded on July 19,2024 at 08:11:44 UTC from IEEE Xplore. Restrictions apply.

A. Load-Aware User Association

In accordance with the load distribution in the centralized algorithm, the motivation of the load-aware user association is to fully exploit the service capability of each BS to improve MUs' transmission rates. The whole operating process is elaborated as follows. On the BS side, each BS n calculates its surplus resource y_n^{res} according to its current traffic demand, i.e.,

$$y_n^{\mathrm{res}} = 1 - \sum_{m \in \mathcal{U}} x_{n,m} R_m^{\mathrm{req}} / \bar{R}_{n,m}. \tag{17}$$

Then, BS n broadcasts y_n^{res} to MUs on a common control channel with its maximum transmission power. On the MU side, each MU m detects the load condition of adjacent BSs by receiving $\{y_n^{\mathrm{res}}\}$ and calculates the potential data rate $R_{n,m}^{\mathrm{pot}}$ that the BS n can provide for it, where

$$R_{n,m}^{\mathrm{pot}} = \begin{cases} R_m^{\mathrm{req}} + y_n^{\mathrm{res}} \bar{R}_{n,m}, & \text{if } x_{n,m} = 1 \\ y_n^{\mathrm{res}} \bar{R}_{n,m}, & \text{if } x_{n,m} = 0. \end{cases} \tag{18}$$

Based on (18), MU m attempts to switch to the BS with the maximum potential data rate for it. Along with the variations of the user association status, a new round of operations will be executed at MUs and BSs, which is repeated until reaching a steady state.

While executing multiple user switching concurrently, the load condition of two neighboring BSs may turn into reverse, which results in that some cell-edge users will switch back and forth between these two BSs. To avoid the ping-pong process, we impose a new user switching regulation whereby each BS allows only one MU's departure and, at the same time, accepts only one MU's access at a time. In actual implementation, when an MU attempts to switch from one BS to another, it needs to send a leave application to the incumbent BS. After receiving the acknowledgment (ACK) from this BS, it then transmits an access request containing its rate requirement to the objective BS. It is only after acquiring ACK once again from the later BS that this handover process is completed; otherwise, the MU will remain in the former BS. On the BS side, each BS collects the leave applications of MUs served by it and chooses that occupying the most resource from it to send ACK. Meanwhile, each BS collects the access requests from outer MUs and only responds to the MU asking for the least resource from it with ACK. This way, the ping-pong process can be avoided.

B. Intracell Power and Resource Allocation

When the user association status remains stable, each BS can adjust its transmission power and update its resource allocation to cater for the new traffic demand. Similar with the energy configuration phase in the centralized algorithm, the power and resource allocation in the distributed algorithm aims to minimize the total energy consumption of the whole system, which is formulated as

$$\min_{\mathbf{P},\mathbf{Y}} \sum_{n \in \mathcal{B}} \rho_n P_n^t$$
$$\text{s.t. C1, C2, C4, C6.} \tag{19}$$

To tackle (19) in a distributed manner, we propose an iterative power and resource allocation scheme, which draws lessons from the IPC. In particular, each BS n first obtains the information on the interference $\{I_{n,m}(\mathbf{P})\}$ received by the MUs associated with it. Then, based on this information, each BS n employes Algorithm 5 to modify its control policy $\{P_n, \mathbf{y}_n\}$ independently. With the update of the transmission power, the interference condition of each MU changes correspondingly so that the control policy of power and resource allocation should be repeatedly updated until the transmission power of each BS remains unchanged.

Theorem 4: The proposed distributed power and resource allocation scheme converges to the global optimum of (19) both synchronously and asynchronously.

Proof: See Appendix C. ■

Algorithm 5 Bisection-based power and resource allocation algorithm (BPRA)

1: **Initialization**: Set the maximum tolerance $\varepsilon_3 > 0$. Set $P_n^l = 0$ and $P_n^u = P_n^{\max}$.
2: **while** 1 **do**
3: $P_n^t = (P_n^l + P_n^u)/2$;
4: Calculate $y_{n,m} = x_{n,m} R_m^{\mathrm{req}} / \overline{R}_{n,m}$ for each m;
5: **if** $1 - \varepsilon_3 < \sum_{m \in \mathcal{U}} y_{n,m} < 1$ **then**
6: Output the control policy $\{P_n, \mathbf{y}_n\}$;
7: break;
8: **else**
9: **if** $\sum_{m \in \mathcal{U}} y_{n,m} > 1$ **then**
10: $P_n^l = P_n^t$;
11: **else**
12: $P_n^u = P_n^t$;
13: **end if**
14: **end if**
15: **end while**

Remark 6: The synchronous iteration requires each BS to acquire real-time information on the interference caused by other BSs and perform power and resource adjustments at the same time. On the contrary, the asynchronous iteration allows BSs to update their control policies with different tempos and perform these updates using outdated information. As a result, a longer time is required by the asynchronous iteration to converge to the fixed point, which will be further discussed by simulations in Section VI-B.

C. Intercell Energy Cooperation

When the transmission power of each BS remains unchanged, the BSs will execute the energy cooperation operations. First, each BS n estimates its energy supply and demand profile, i.e., the comparison between E_n and $\rho_n P_n^t + P_n^c$. In the context of $\rho_n P_n^t + P_n^c < E_n$, BS n will transfer its redundant renewable energy $E_n - \rho_n P_n^t - P_n^c$ to the aggregator; otherwise, BS n will apply for energy $\rho_n P_n^t + P_n^c - E_n$ from the aggregator. After gathering the energy requests from the BSs with renewable energy deficits, the aggregator will utilize the

Authorized licensed use limited to: Huazhong University of Science and Technology. Downloaded on July 19,2024 at 08:11:44 UTC from IEEE Xplore. Restrictions apply.

SWF to allocate the collected renewable energy to these BSs according to their energy demands $(\rho_n P_n^t + P_n^c - E_n)$ and loss factors $(\alpha_{a,n})$.

D. Message Complexity Analysis

In the user association phase, each successful handover requires two rounds of message exchanges, i.e., two request packets and two ACK packets, whereas each failure costs two request packets and one ACK packet at most. With the variation of the load distribution, the corresponding BSs will refresh their surplus resource $\{y_n^{\text{res}}\}$ and broadcast this information to all MUs. In the worst case, all MUs need to hand over from one BS to another, and only one succeeds in each concurrent process; thereby, the fastest handover is attempted only once, and the slowest undergoes $M-1$ failures before the final success. As such, the message complexity in the user association phase is $O(\sum_{K=0}^{M-1}(3K+4)+NM) = O(1.5M^2+2.5M+NM) = O(1.5M^2+NM)$. In the power and resource allocation phase, each BS needs to acquire the interference conditions of the MUs associated with it in each iteration and repeats it until convergence, resulting in the message complexity $O(IM)$, where I is the expected number of iterations. Simulation results show that I is usually smaller than 6. In the energy exchange phase, only energy-inefficient BSs need to send requests to the aggregator to apply for renewable energy, which costs $O(N)$. Therefore, the total message complexity of the distributed control policy is $O((1.5M+I+N)M)$.

VI. Simulation Results

Here, we present abundant simulation results to evaluate the performance of our proposed algorithms. First, we investigate the convergence and the effectiveness of the centralized algorithm by comparing it with the exhaustive search. Then, we discuss the convergence of the distributed power and resource allocation scheme (DPRA) proposed in Section V-B. Finally, we exhibit the performance gain of our proposed algorithms against other related schemes.

The common simulation parameters are set as follows, unless otherwise specified. The scenario is a practical macrocellular network with the distance between two neighboring BSs being 1000 m [21]. The maximum transmission power of all BSs is set to 40 W [25], and their energy-harvesting rates (E_n) are randomly generated in an interval [10, 90] W. Furthermmore, the inefficiency of the power amplifier and the static circuit power consumption of each BS are set to $\rho_n = 2.8571$ and $P_n^c = 10$ W [14]. The total bandwidth of the system is 10 MHz [24], and the loss factors $(\alpha_{n,a})$ and $(\alpha_{a,n})$ are randomly taken values in [0.7, 0.9] [19]. Additionally, the noise power is set to $\eta = 5 \times 10^{-17}$ W/Hz, and the path-loss exponent and the shadow fading standard deviation are supposed to be 4 and 8 dB, respectively. The maximum tolerances are set to $\varepsilon_1 = \varepsilon_2 = \varepsilon_3 = 10^{-2}$.

A. Convergence and Effectiveness of the JESLS

To compare with the exhaustive search, we first conduct simulations in a simple two-cell network. The rate requirements of all MUs are set to the same 3 Mb/s. Fig. 2 shows the convergence of the JESLS in which the simulation result for each given number of users is a random realization. As shown, the total grid power consumption always descends after each iteration until convergence because the JESLS maximizes the redundant transmission rates of all MUs in each iteration by performing user association and resource allocation, which exploits the service capability of each BS. Then, the total grid power consumption can be reduced by appropriate power control and energy transfer. In addition, the total grid power consumption is lower bounded by the optimal objective value of (3); thus, the JESLS can always converge after finite iterations. In fact, it is shown in Fig. 2 that the number of iterations is usually no more than eight, which reflects the convergent validity of our proposed algorithm.

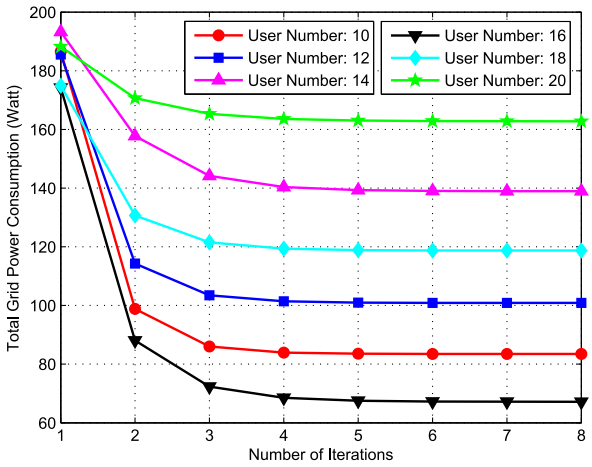

Fig. 2. Convergence evolution of the centralized algorithm.

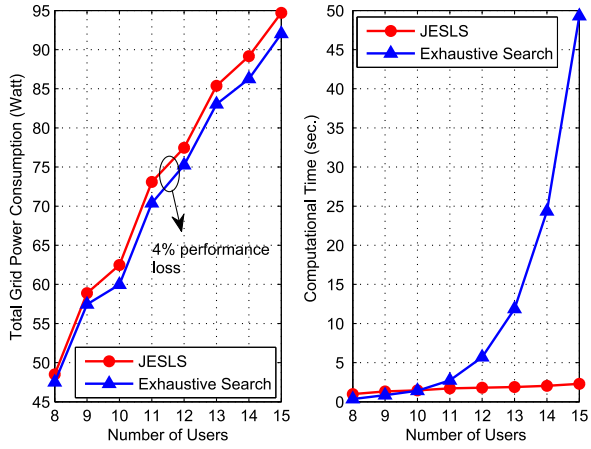

Fig. 3. Effectiveness exhibition of the centralized algorithm.

Fig. 3 shows the performance and complexity comparisons between the JESLS and exhaustive search. The resulting values are obtained by averaging over 1000 random realizations. Compared with the exhaustive search, we can observe that the JESLS saves significant computational time at the expense of slight performance degradation. The performance loss of the JESLS with respect to the optimal value is only about 4% and independent of the number of MUs, which indicates that

Authorized licensed use limited to: Huazhong University of Science and Technology. Downloaded on July 19,2024 at 08:11:44 UTC from IEEE Xplore. Restrictions apply.

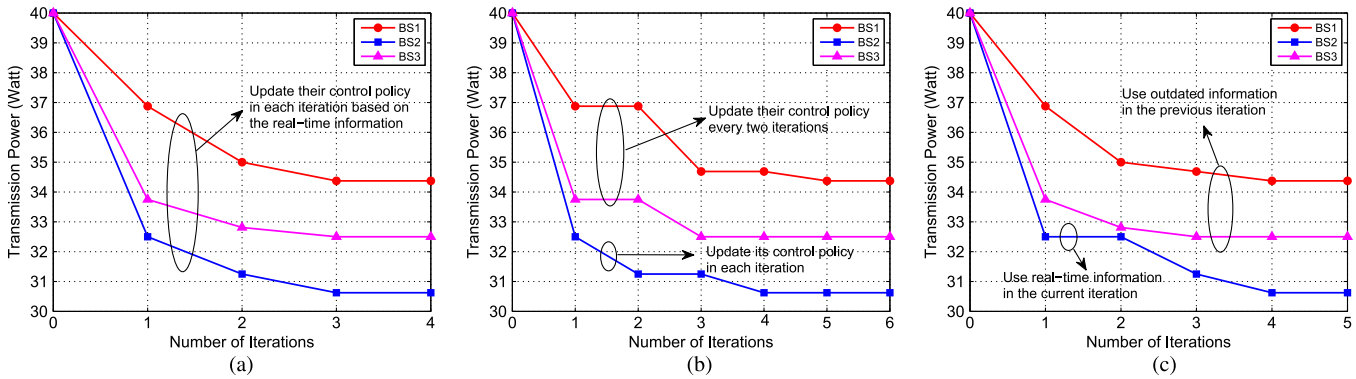

Fig. 4. Convergence evolution of the distributed power and resource allocation scheme. (a) DPRA-SP: synchronous policy based on real-time information. (b) DPRA-DR: asynchronous policy with different iteration rates. (c) DPRA-OI: asynchronous policy with outdated information.

the JESLS is performance stable. Furthermore, the complexity comparison shows that the computational time of the exhaustive search increases with the number of MUs by exponential law, limiting it to be applied into large-scale networks. In contrast, our proposed algorithm costs only a brief computational time, even with large MUs, which reflects that the JESLS has good scalability.

B. Convergence of the DPRA

We investigate the convergence of the DPRA proposed in Section V-B. To demonstrate the simulation results clearly, we conduct simulations in a three-cell cluster, which is identical with that in Fig. 5. Moreover, 50 MUs are uniformly distributed in this network with rate requirements randomly generated in [0.5, 1.0] Mb/s. We discuss three types of the DPRA, namely, synchronous policy (DPRA-SP), asynchronous policy with different iteration rates (DPRA-DR), and asynchronous policy with outdated information (DPRA-OI), which are presented in Fig. 4(a)–(c), respectively. The DPRA-SP requires each BS to perform power and resource allocation simultaneously based on real-time information. In the DPRA-DR, BS 2 updates its control policy in each iteration, whereas BS 1 and BS 3 do these every two iterations. In the DPRA-OI, BS 1 and BS 3 utilize the outdated information in the previous iteration, and BS 2 utilizes real-time information in the current iteration. The simulation results for these three control polices are random realizations under the same parameter settings.

From the simulation results, we note that all these three control polices converge to the same fixed point quickly, which is consistent with Theorem 4. The transmission power of each BS in the DPRA-SP always descends in each iteration, and its convergence rate is the fastest because each BS executes power and resource adjustment in real time and synchronously. However, additional synchronization overhead is required by the DPRA-SP to coordinate all BSs in concurrent policy updating. Compared with the synchronous policy, more time is expended by the DPRA-DR and DPRA-OI to reach the steady state. In spite of this, the asynchronous policies are more easily implemented in practice due to their flexible operational forms. Additionally, it is shown in Fig. 4 that the decline of each BS's transmission power is mainly concentrated on the first three iterations; therefore, we can strike a balance between the performance and overhead by controlling the iteration numbers in practical systems.

C. Performance Comparison

Here, we evaluate the performance of our algorithms by comparing them with other related schemes. For notational simplicity, our proposed distributed control policy is denoted as DJESLS. We compare our algorithms with two other centralized schemes: MEB, which is without energy sharing, and OEC, which is without load shifting. The MEB proposed in [18] balances the energy consumption among BSs via cell size adaptation (i.e., optimizing the load distribution) and thereby reduces the total grid energy consumption. The OEC is the offline energy cooperation scheme devised in [19], which minimizes the total grid energy consumption by means of energy cooperation.

We first present a special case to study the operational mechanisms of the OEC, MEB, and JESLS. The considered scenario is shown in Fig. 5 with three BSs and ten MUs in which the channel power gains between BSs and MUs are given in Table I. The energy harvesting rate of each BS is set as $E_1 = 25$ W, $E_2 = 40$ W, and $E_3 = 70$ W. Moreover, the rate requirements of all MUs are 0.5 Mb/s, and the loss factors (i.e., $\alpha_{n,a}$ and $\alpha_{a,n}$, n = 1, 2, 3) are the same $\alpha = 0.8$.

As shown in Fig. 5(a), the power consumption of different BSs in the OEC is seriously unbalanced due to the unbalanced load distribution, which results in large energy consumption at BS 1. Although the renewable energy of BS 1 is enhanced by obtaining the energy from BS 2 and BS 3, partial energy is wasted during the energy transfer procedure, and a large energy deficit still occurs at BS 1, leading to 22-J grid energy consumption. In the MEB, the energy consumption of different BSs is balanced to some extent through offloading some mobile traffic from BS 1 to BS 2 and BS 3. However, renewable energy is still underutilized, since the energy harvesting rates are various among different BSs, and load shifting can only be utilized for cell-edge users. As a consequence, the renewable energy at BS 1 and BS 2 is insufficient, whereas the renewable energy at BS 3 is superfluous (30-J renewable energy is wasted), finally causing 41-J grid energy consumption. By jointly optimizing

Authorized licensed use limited to: Huazhong University of Science and Technology. Downloaded on July 19,2024 at 08:11:44 UTC from IEEE Xplore. Restrictions apply.

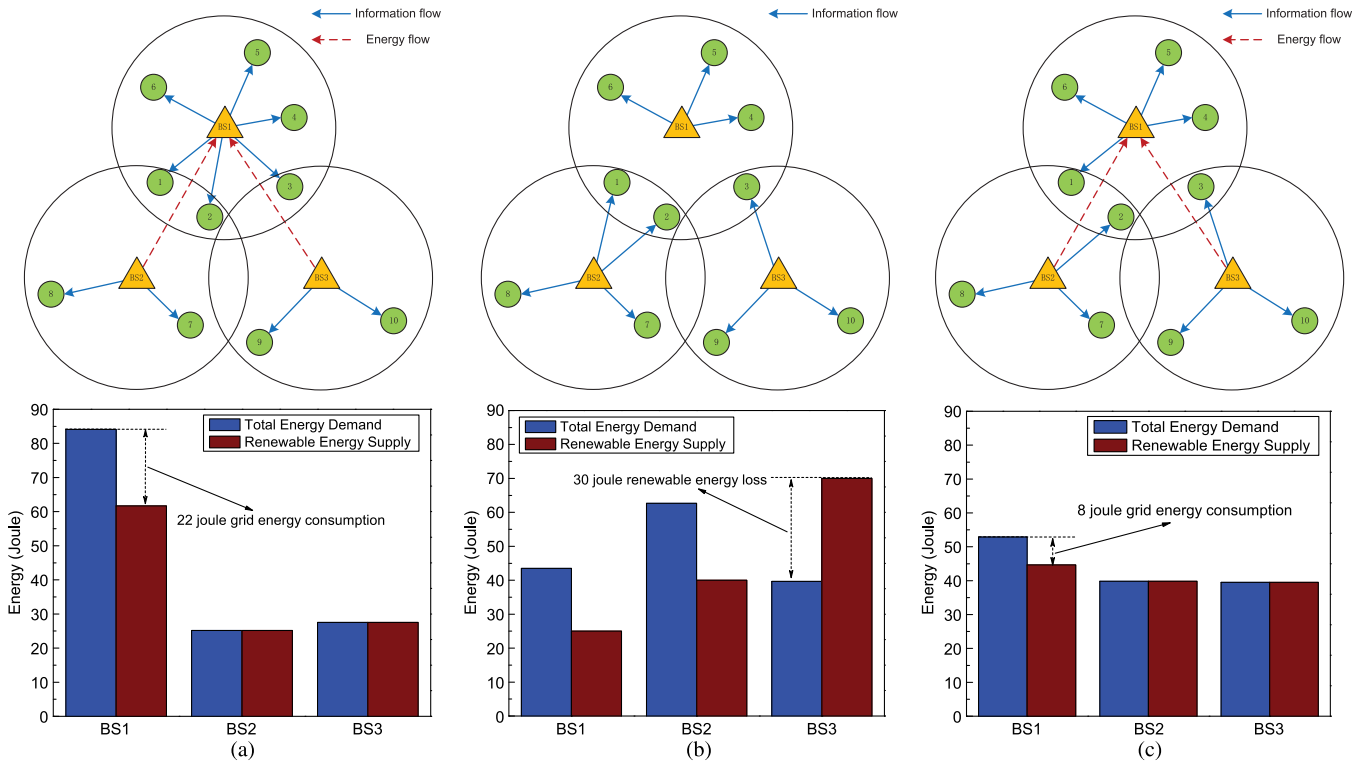

Fig. 5. Case study on the operational mechanisms of different algorithms. (a) OEC: offline energy cooperation scheme without load shifting. (b) MEB: multi-BSs energy balancing scheme without energy sharing. (c) JESLS: jointly optimizing energy sharing and load shifting scheme.

TABLE I
SETTINGS FOR THE CHANNEL POWER GAIN

Channel power gain (10^{-12})	MU1	MU2	MU3	MU4	MU5
BS1	6.26	6.53	5.32	4.08	4.83
BS2	2.85	4.26	0.477	0.205	0.299
BS3	0.168	0.874	4.95	0.148	0.291
Channel power gain (10^{-12})	MU6	MU7	MU8	MU9	MU10
BS1	5.62	0.101	0.117	0.139	0.198
BS2	0.141	9.34	5.67	0.172	0.783
BS3	0.781	0.57	0.345	5.69	6.74

the energy sharing and load shifting among BSs, both the traffic load and renewable energy are balanced by our proposed JESLS, as shown in Fig. 5(c). Correspondingly, the total energy demand and renewable energy supply at each BS are well matched, and hence only 8-J grid energy is required for the whole network.

Then, we conduct simulations in a random network with a seven-cell wrap-around topology in which the rate requirements of all MUs are randomly taken values in [0.5, 1.0] Mb/s. All simulation results are obtained by averaging over 1000 simulation runs. Fig. 6 shows total grid power consumption versus number of MUs. As shown, our proposed algorithms outperform the OEC and MEB in terms of grid power consumption. The main reasons are twofold: On the one hand, load shifting balances the energy consumption among BSs, and the corresponding intercell interference coordination degrades each BS's transmission power. Thus, less energy demand is required by our algorithms than the OEC, which is verified in Fig. 7. On the other hand, energy sharing mitigates the differences in the energy harvesting rates of BSs and thereby greatly reduces the unnecessary energy waste in the BSs with

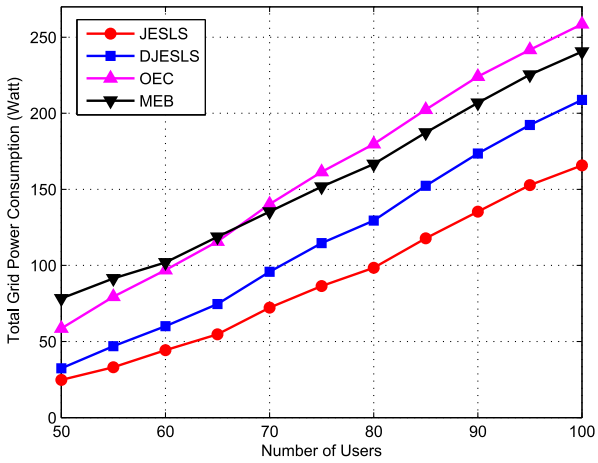

Fig. 6. Total grid power consumption versus number of MUs.

surplus renewable energy but small traffic demand. As such, our algorithms can make better use of the renewable energy than the MEB, which is confirmed in Fig. 8. To sum up, high-efficiency utilization for the renewable energy and low energy demand jointly contribute to the performance improvement of our proposed algorithms. In addition, the JESLS consumes less grid power with respect to the DJESLS. The reason is that the centralized algorithm achieves a better match between the renewable energy and traffic load by performing multiple load and energy coordinations, and in consequence, it can use lower transmission power to meet the rate requirements of all MUs, as shown in Fig. 7.

Authorized licensed use limited to: Huazhong University of Science and Technology. Downloaded on July 19,2024 at 08:11:44 UTC from IEEE Xplore. Restrictions apply.

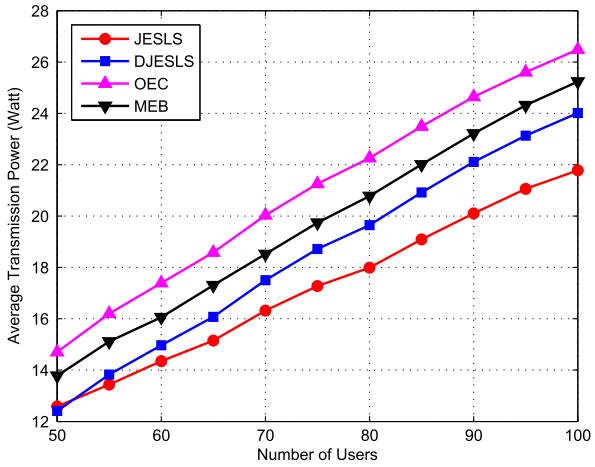

Fig. 7. Average transmission power versus number of MUs.

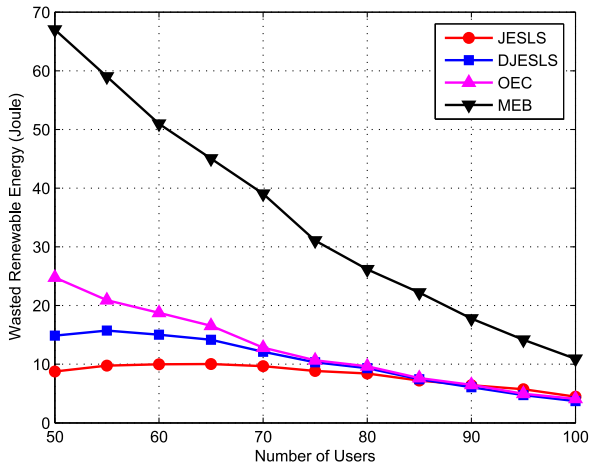

Fig. 8. Wasted renewable energy versus number of MUs.

As shown in Fig. 7, the average transmission power significantly increases with the number of MUs. This is because with the increase in MUs, each BS will support a more heavy load, i.e., serving more MUs. Furthermore, Lemma 3 indicates that the optimal control policy that minimizes each BS's energy consumption must satisfy the condition $\sum_{m\in\mathcal{U}} y_{n,m} = 1$; that is, all communication resources (time slot or frequency band) are allocated to its served MUs. Accordingly, the communication resource obtained by each MU decreases with the number of MUs. To meet the rate requirement of all MUs, the BS has to improve its transmission power to enlarge each MU's instantaneous transmission rate. Due to this reason, the average transmission power significantly increases with the number of MUs.

Fig. 8 shows the wasted renewable energy E_R^{was} versus MU number, and E_R^{was} is defined as

$$E_R^{\text{was}} = \begin{cases} \sum\limits_{n\in\mathcal{B}} E_n - \sum\limits_{n\in\mathcal{B}} \xi_n, & \text{if } P_G^{\text{tot}} > 0 \\ 0, & \text{otherwise} \end{cases}. \quad (20)$$

Note that the wasted renewable energy of the OEC and our algorithms are caused by the resistive loss and processing overhead in the energy transfer processes, whereas that of the MEB is due to that some harvested energy is not run out of in time by some BSs. It is observed that the renewable energy is better utilized by the OEC and our algorithms, since energy cooperation exploits the spatial diversity of the renewable energy more effectively and hence mitigates the energy harvesting fluctuations. However, the achieved gains decrease with the number of MUs, since more energy is required by each BS with the increasing of the traffic load; as a result, the case of energy transfer among BSs occurs less. This also accounts for the power gap between the MEB and OEC narrowing and going into reverse with the increasing of MUs, as shown in Fig. 6. However, by jointly optimizing the load and energy distribution, our proposed algorithms can still save more grid power in comparison to the OEC, even with large MUs. Thus, our proposed algorithms can fully exploit the renewable energy to reduce the total grid energy consumption.

VII. Conclusion

In this paper, we have addressed the grid energy conservation problem by jointly considering energy sharing and load shifting in a hybrid-energy-powered cellular network. We have first devised a cost-efficient centralized algorithm to tackle the hard problem, which solves the LDP and the ECP iteratively until convergence. Based on the centralized algorithm, we have further proposed a three-phase distributed control policy, which can be flexibly executed at MUs and BSs only with their local information. Simulation results have verified the convergence and effectiveness of our proposed algorithms. Our results provide both theoretical and practical guidelines for the design of a green communication system incorporated with energy harvesting and smart grid.

Appendix A
Proof of Lemma 2

Let $\{\mathbf{P}^*, \mathbf{E}^*\}$ denote the control policy obtained by solving (12) and (13) sequentially. Then, we prove Lemma 2 by contradiction. Specifically, assume that there is another control policy $\{\mathbf{P}', \mathbf{E}'\}$ outperforming $\{\mathbf{P}^*, \mathbf{E}^*\}$, i.e., $P_G^{\text{tot}}(\mathbf{P}', \mathbf{E}') < P_G^{\text{tot}}(\mathbf{P}^*, \mathbf{E}^*)$. In what follows, we will prove that this control policy is nonexistent in three cases.

1) $P_n' \le P_n^* \,\forall\, n$ and $\mathbf{P}' \ne \mathbf{P}^*$.
   This situation cannot happen since it will lead to $\sum_{n\in\mathcal{B}} \rho_n P_n' < \sum_{n\in\mathcal{B}} \rho_n P_n^*$, which contradicts the minimality of the objective function in (12).
2) $P_n' \ge P_n^* \,\forall\, n$ and $\mathbf{P}' \ne \mathbf{P}^*$.
   For this energy configuration, we can get the following inequation:

$$\sum_{n\in\mathcal{B}} (\rho_n P_n' + P_n^c - \xi_n') \overset{(a)}{>} \sum_{n\in\mathcal{B}} (\rho_n P_n^* + P_n^c - \xi_n')^+ \overset{(b)}{\ge} \sum_{n\in\mathcal{B}} (\rho_n P_n^* + P_n^c - \xi_n^*) \quad (21)$$

where inequation (a) is due to that with the same available renewable energy, reducing the transmission power of

Authorized licensed use limited to: Huazhong University of Science and Technology. Downloaded on July 19,2024 at 08:11:44 UTC from IEEE Xplore. Restrictions apply.

each BS can degrade the total grid energy cost. Inequation (b) is satisfied for the reason that ξ^* is the optimal energy cooperation scheme without energy waste for $\mathbf{P}^*$, that is, $\xi_n^* \le \rho_n P_n^* + P_n^c \; \forall\, n$.

3) $P_i' \le P_i^* \;\; \forall\, i \in \mathcal{B}_1$, $P_j' \ge P_j^* \;\; \forall j \in \mathcal{B}_2$, and $\mathbf{P}' \ne \mathbf{P}^*$, where $\mathcal{B}_1 \cap \mathcal{B}_2 = \emptyset$, and $\mathcal{B}_1 \cup \mathcal{B}_2 = \mathcal{B}$.

If 3) is true, we can always find a new transmission power configuration scheme $\mathbf{P}''$ defined as

$$P_n'' = \min\left(P_n', P_n^*\right) = \begin{cases} P_n', & \text{if } n \in \mathcal{B}_1 \\ P_n^*, & \text{if } n \in \mathcal{B}_2 \end{cases}. \tag{22}$$

As such, $\mathbf{P}''$ must satisfy C6 in (12).

If $x_{n,m} = 1$ and $n \in \mathcal{B}_1$, the transmission rate of MU m is given by

$$\begin{aligned} R_m &= y_{n,m} \log_2 \left(1 + \frac{P_n' g_{n,m}}{\sum\limits_{i \ne n, i \in \mathcal{B}_1} P_i' g_{i,m} + \sum\limits_{j \in \mathcal{B}_2} P_j^* g_{j,m} + \eta_m}\right) \\ &\ge y_{n,m} \log_2 \left(1 + \frac{P_n' g_{n,m}}{\sum\limits_{i \ne n, i \in \mathcal{B}_1} P_i' g_{i,m} + \sum\limits_{j \in \mathcal{B}_2} P_j' g_{j,m} + \eta_m}\right) \\ &\ge R_m^{\text{req}}. \end{aligned} \tag{23}$$

Similarly, if $x_{n,m} = 1$ and $n \in \mathcal{B}_2$, the transmission rate of MU m is shown as

$$\begin{aligned} R_m &= y_{n,m} \log_2 \left(1 + \frac{P_n^* g_{n,m}}{\sum\limits_{i \in \mathcal{B}_1} P_i' g_{i,m} + \sum\limits_{j \ne n, j \in \mathcal{B}_2} P_j^* g_{j,m} + \eta_m}\right) \\ &\ge y_{n,m} \log_2 \left(1 + \frac{P_n^* g_{n,m}}{\sum\limits_{i \in \mathcal{B}_1} P_i^* g_{i,m} + \sum\limits_{j \ne n, j \in \mathcal{B}_2} P_j^* g_{j,m} + \eta_m}\right) \\ &\ge R_m^{\text{req}}. \end{aligned} \tag{24}$$

According to (23) and (24), $\mathbf{P}''$ also satisfies C1 in (12). Therefore, $\mathbf{P}''$ is also a feasible solution of (12) but satisfies

$$\sum_{n \in \mathcal{B}} \rho_n P_n'' = \sum_{i \in \mathcal{B}_1} \rho_n P_i' + \sum_{j \in \mathcal{B}_2} \rho_n P_j^* < \sum_{n \in \mathcal{B}} \rho_n P_n^* \tag{25}$$

which contradicts the minimality of $\mathbf{P}^*$ for (12). Therefore, we can know that $\mathbf{P}''$ is nonexistent, and hence condition 3) is nonexistent as well.

To sum up, we conclude that the optimal solution of (11) can be obtained by solving (12) and (13) sequentially, which completes the proof of Lemma 2.

APPENDIX B
PROOF OF THEOREM 3

To prove that $T_n(\mathbf{P})$ is a standard interference function, we need to verify that it satisfies the following three properties [32].

1) Positivity: $T_n(\mathbf{P}) > 0$.
2) Monotonicity: If $\mathbf{P} \ge \mathbf{P}'$, then $T_n(\mathbf{P}) \ge T_n(\mathbf{P}')$.
3) Scalability: For all $\theta > 1$, $\theta T_n(\mathbf{P}) > T_n(\theta \mathbf{P})$.

It can be easily verified that $\max_{m \in \mathcal{U}} \; f_{n,m}(\mathbf{P}) > 0$, thus $T_n(\mathbf{P}) = \max_{m \in \mathcal{U}} \; f_{n,m}(\mathbf{P}) > 0$.

If $\mathbf{P} \ge \mathbf{P}'$, we have $f_{n,m}(\mathbf{P}) \ge f_{n,m}(\mathbf{P}')$ on account of $I_{n,m}(\mathbf{P}) \ge I_{n,m}(\mathbf{P}')$. Furthermore, let $m^* = \arg\max\limits_{m \in \mathcal{U}} f_{n,m}(\mathbf{P}')$, and then, we get

$$\begin{aligned} T_n(\mathbf{P}') &= \max_{m \in \mathcal{U}} f_{n,m}(\mathbf{P}') \\ &= f_{n,m^*}(\mathbf{P}') \\ &\le f_{n,m^*}(\mathbf{P}) \\ &\le \max_{m \in \mathcal{U}} f_{n,m}(\mathbf{P}) = T_n(\mathbf{P}). \end{aligned} \tag{26}$$

Therefore, $T_n(\mathbf{P}) \ge T_n(\mathbf{P}')$ for $\mathbf{P} \ge \mathbf{P}'$, which verifies its monotonicity.

Similarly, for all $\theta > 1$, we get $\theta f_{n,m}(\mathbf{P}) > f_{n,m}(\theta \mathbf{P})$ due to the existence of the nonzero noise power. Furthermore, we denote $m^* = \arg\max\limits_{m \in \mathcal{U}} f_{n,m}(\theta \mathbf{P})$ and have

$$\begin{aligned} T_n(\theta \mathbf{P}) &= \max_{m \in \mathcal{U}} f_{n,m}(\theta \mathbf{P}) \\ &= f_{n,m^*}(\theta \mathbf{P}) \\ &< \theta f_{n,m^*}(\mathbf{P}) \\ &\le \max_{m \in \mathcal{U}} \theta f_{n,m}(\mathbf{P}) = \theta T_n(\mathbf{P}). \end{aligned} \tag{27}$$

Thus, $\theta T_n(\mathbf{P}) > T_n(\theta \mathbf{P})$ for all $\theta > 1$, which proves its scalability.

Now, we complete the proof of Theorem 3.

APPENDIX C
PROOF OF THEOREM 4

Primarily, we decompose (19) into N subproblems, each of which corresponds to one BS and is formulated as

$$\begin{aligned} \min_{P_n^t, \mathbf{y}_n} \;\; & P_n^t \\ \text{s.t. C1}: \;\; & y_{n,m} \overline{R}_{n,m} \ge x_{n,m} R_m^{\text{req}} \; \forall\, m \\ \text{C2}: \;\; & \sum_{m \in \mathcal{U}} y_{n,m} \le 1 \\ \text{C4}: \;\; & 0 \le y_{n,m} \le x_{n,m} \; \forall\, m \\ \text{C6}: \;\; & 0 \le P_n^t \le P_n^{\max}. \end{aligned} \tag{28}$$

As shown, the objective value of (28) for BS n is closely related to other BSs' transmission power. For convenience, we denote $\Gamma_n(\mathbf{P})$ as the minimum objective value subject to all constraints in (28). In the later part, we will prove that $\Gamma_n(\mathbf{P})$ is a standard interference function. Before this, we first confirm that $\Gamma_n(\mathbf{P})$ can be achieved by our proposed BPRA.

Authorized licensed use limited to: Huazhong University of Science and Technology. Downloaded on July 19,2024 at 08:11:44 UTC from IEEE Xplore. Restrictions apply.

Lemma 3: The sufficient and necessary condition to achieve the global optimum of (28) is $y_{n,m}\overline{R}_{n,m} = x_{n,m}R_m^{\mathrm{req}}\ \forall m$ and $\sum_{m\in\mathcal{U}} y_{n,m} = 1$, that is, C1 and C2 are tight at optimality of (28).

Proof: We first prove the necessity by contradiction. Assume that C1 is not tight at optimality, i.e., $y_{n,m}\overline{R}_{n,m} > x_{n,m}R_m^{\mathrm{req}}$ for all or partial MUs. In the context of $y_{n,m}\overline{R}_{n,m} > x_{n,m}R_m^{\mathrm{req}}\ \forall m$, we can obviously reduce each P_n without violating any constraints in (28). For the other condition, we can make all MUs' transmission rates larger than their own demands by shifting some redundant resource of the MUs with $y_{n,m}\overline{R}_{n,m} > x_{n,m}R_m^{\mathrm{req}}$ to the others, which is transformed into the first case, and thus it is also not optimal. Additionally, if C2 is not tight, i.e., $\sum_{m\in\mathcal{U}} y_{n,m} < 1$, we can allocate the vacant resource to all MUs to improve their transmission rates. As such, their transmission rates are also larger than their own demands, and hence $\sum_{m\in\mathcal{U}} y_{n,m} < 1$ is not the optimal condition as well. Now, we have confirmed the necessity.

Next, we prove the sufficiency. Rearranging C1 in (28), we can get

$$P_n^t \geq \frac{\sum\limits_{n'\in\mathcal{B},n'\neq n} P_{n'}^t g_{n',m} + \eta_m}{g_{n,m}} \left(2^{\frac{R_m^{\mathrm{req}}}{W y_{n,m}}} - 1\right)\ \forall m. \quad (29)$$

Therefore, the minimum transmission power of BS n can be expressed as

$$\begin{aligned} P_n^{\min} &= \max_{m\in\mathcal{U}} \frac{\sum\limits_{n'\in\mathcal{B},n'\neq n} P_{n'}^t g_{n',m} + \eta_m}{g_{n,m}} \left(2^{\frac{R_m^{\mathrm{req}}}{W y_{n,m}}} - 1\right) \\ &= \frac{\sum\limits_{n'\in\mathcal{B},n'\neq n} P_{n'}^t g_{n',m^*} + \eta_{m^*}}{g_{n,m^*}} \left(2^{\frac{R_m^{\mathrm{req}}}{W y_{n,m^*}}} - 1\right) \quad (30) \end{aligned}$$

where m^* denotes the MU that determines the maximum transmission power of BS n.

Note that (30) indicates that the minimum transmission power just satisfies the rate requirement of MU m^*, i.e., $y_{n,m^*}\overline{R}_{n,m^*} = x_{n,m^*}R_{m^*}^{\mathrm{req}}$. Furthermore, we can find that $P_n^{\min}$ is strictly monotonically decreasing in y_{n,m^*}. To maximize y_{n,m^*} (i.e., minimize $P_n^{\min}$), the resource allocation the policy must satisfy $y_{n,m}\overline{R}_{n,m} = x_{n,m}R_m^{\mathrm{req}}\ \forall m \neq m^*$, and $\sum_{m\in\mathcal{U}} y_{n,m} = 1$. Now, sufficiency is proved. ■

According to Lemma 3, $\Gamma_n(\mathbf{P})$ can be obtained by our proposed BPRA, as the sufficient condition is achieved at the termination of the BPRA.

Lemma 4: $\Gamma_n(\mathbf{P})$ is a standard interference function.

Proof: Similar with the proof of Theorem 3, we only need to verify that $\Gamma_n(\mathbf{P})$ holds the properties of positivity, monotonicity, and scalability.

Due to the existence of noise and interference, $\Gamma_n(\mathbf{P})$ is always larger than zero, proving its positivity.

Comparing the definitions of $T_n(\mathbf{P})$ and $\Gamma_n(\mathbf{P})$, we can find that $\Gamma_n(\mathbf{P})$ is the improvement of $T_n(\mathbf{P})$ by further optimizing $\mathbf{y}_n$. Thus, we can express $\Gamma_n(\mathbf{P})$ as

$$\Gamma_n(\mathbf{P}) = \min_{\mathbf{y}_n} T_n(\mathbf{P}, \mathbf{y}_n). \quad (31)$$

Then, the following inequation for $\mathbf{P} \geq \mathbf{P}'$ can be obtained:

$$\begin{aligned} \Gamma_n(\mathbf{P}) &= \min_{\mathbf{y}_n} T_n(\mathbf{P}, \mathbf{y}_n) \\ &= T_n\left(\mathbf{P}, \mathbf{y}_n^*\right) \\ &\overset{(a)}{\geq} T_n\left(\mathbf{P}', \mathbf{y}_n^*\right) \\ &\geq \min_{\mathbf{y}_n}\ T_n(\mathbf{P}', \mathbf{y}_n) = \Gamma_n(\mathbf{P}') \quad (32) \end{aligned}$$

where $\mathbf{y}_n^* = \arg\min_{\mathbf{y}_n}\ T_n(\mathbf{P}, \mathbf{y}_n)$, and (a) is satisfied due to the monotonicity of $T_n(\mathbf{P})$. Hence, $\Gamma_n(\mathbf{P})$ also has the monotonic property.

Furthermore, for all $\theta > 1$, we have

$$\begin{aligned} \theta\Gamma_n(\mathbf{P}) &= \theta \min_{\mathbf{y}_n}\ T_n(\mathbf{P}, \mathbf{y}_n) \\ &= \theta T_n\left(\mathbf{P}, \mathbf{y}_n^*\right) \\ &\overset{(b)}{>} T_n\left(\theta\mathbf{P}, \mathbf{y}_n^*\right) \\ &\geq \min_{\mathbf{y}_n}\ T_n(\theta\mathbf{P}, \mathbf{y}_n) = \Gamma_n(\theta\mathbf{P}) \quad (33) \end{aligned}$$

where (b) holds due to the scalability of $T_n(\mathbf{P})$. Therefore, $\Gamma_n(\mathbf{P})$ also preserves the scalability.

To sum up, we prove that $\Gamma_n(\mathbf{P})$ is a standard interference function. ■

In light of the standard interference function [32], [33], our proposed distributed power and resource allocation scheme can converge to the global optimum of (19) both synchronously and asynchronously.

To this end, we complete the proof of Theorem 4 in this paper.

REFERENCES

[1] Y. Chen, S. Zhang, S. Xu, and G. Li, "Fundamental trade-offs on green wireless networks," *IEEE Commun. Mag.*, vol. 49, no. 6, pp. 30–37, Jun. 2011.

[2] E. Oh, B. Krishnamachari, X. Liu, and Z. Niu, "Toward dynamic energy-efficient operation of cellular network infrastructure," *IEEE Commun. Mag.*, vol. 49, no. 6, pp. 56–61, Jun. 2011.

[3] D. Feng *et al.*, "A survey of energy-efficient wireless communications," *IEEE Commun. Surveys Tut.*, vol. 15, no. 1, pp. 167–178, 1st Quart. 2013.

[4] J. G. Andrews *et al.*, "What will 5G be?" *IEEE J. Sel. Areas Commun.*, vol. 32, no. 6, pp. 1065–1082, Jun. 2014.

[5] Z. Hasan, H. Boostanimehr, and V. Bhargava, "Green cellular networks: A survey, some research issues and challenges," *IEEE Commun. Surveys Tut.*, vol. 13, no. 4, pp. 524–540, Nov. 2011.

[6] S. Luo, R. Zhang, and T. J. Lim, "Joint transmitter and receiver energy minimization in multiuser OFDM systems," *IEEE Trans. Commun.*, vol. 62, no. 10, pp. 3504–3516, Oct. 2014.

[7] S. Zhou, J. Gong, Z. Yang, Z. Niu, and P. Yang, "Green mobile access network with dynamic base station energy saving," in *Proc. ACM MobiCom*, Beijing, China, Sep. 2009, pp. 20–25.

[8] S. Bhaumik, G. Narlikar, S. Chattopadhyay, and S. Kanugovi, "Breathe to stay cool: Adjusting cell sizes to reduce energy consumption," in *Proc. ACM SIGCOMM Workshop Green Netw.*, New York, NY, USA, Aug. 2010, pp. 41–46.

[9] T. Han and N. Ansari, "Powering mobile networks with green energy," *IEEE Wireless Commun.*, vol. 21, no. 1, pp. 90–96, Feb. 2014.

Authorized licensed use limited to: Huazhong University of Science and Technology. Downloaded on July 19,2024 at 08:11:44 UTC from IEEE Xplore. Restrictions apply.

[10] Huawei, Mobile Networks Go Green. [Online]. Available: http://www.huawei.com/en/about-huawei/publications/communicaite/hw-082734.htm
[11] "Sustainable energy use in mobile communications," Ericsson Inc., Stockholm, Sweden, Tech. paper, Aug. 2007.
[12] E-Plus, Nokia Siemens Networks Build Germany's First Off-Grid Base Station. [Online]. Available: http://networks.nokia.com/news-events/press-room/press-releases/e-plus-nokia-siemens-networks-build-germany-s-first-off-grid-base-station
[13] J. Gong, S. Zhou, and Z. Niu, "Optimal power allocation for energy harvesting and power grid coexisting wireless communication systems," *IEEE Trans. Commun.*, vol. 61, no. 7, pp. 3040–3049, Jul. 2013.
[14] D. Ng, E. Lo, and R. Schober, "Energy-efficient resource allocation in OFDMA systems with hybrid energy harvesting base station," *IEEE Trans. Wireless Commun.*, vol. 12, no. 7, pp. 3412–3427, Jul. 2013.
[15] J. Gong, S. Zhou, Z. Niu, and J. Thompson, "Energy-aware resource allocation for energy harvesting wireless communication systems," in *Proc. IEEE VTC—Spring*, Dresden, Germany, Jun. 2013, pp. 1–5.
[16] J. Zhou, M. Li, L. Liu, X. She, and L. Chen, "Energy source aware target cell selection and coverage optimization for power saving in cellular networks," in *Proc. IEEE GreenCom-CPSCom*, HangZhou, China, Dec. 2010, pp. 1–8.
[17] T. Han and N. Ansari, "ICE: Intelligent cell breathing to optimize the utilization of green energy," *IEEE Commun. Lett.*, vol. 16, no. 6, pp. 866–869, Jun. 2012.
[18] T. Han and N. Ansari, "On optimizing green energy utilization for cellular networks with hybrid energy supplies," *IEEE Trans. Wireless Commun.*, vol. 12, no. 8, pp. 3872–3882, Aug. 2013.
[19] Y.-K. Chia, S. Sun, and R. Zhang, "Energy cooperation in cellular networks with renewable powered base stations," *IEEE Trans. Wireless Commun.*, vol. 13, no. 12, pp. 6996–7010, Dec. 2014.
[20] Y. Guo, J. Xu, L. Duan, and R. Zhang, "Joint energy and spectrum cooperation for cellular communication systems," *IEEE Trans. Commun.*, vol. 62, no. 10, pp. 3678–3691, Oct. 2014.
[21] J. Xu and R. Zhang, "CoMP meets smart grid: A new communication and energy cooperation paradigm," *IEEE Trans. Veh. Technol.*, vol. 64, no. 6, pp. 2476–2488, Jun. 2015.
[22] J. Xu and R. Zhang, "Cooperative energy trading in CoMP systems powered by smart grids," *IEEE Trans. Veh. Technol.*, vol. 65, no. 4, pp. 2142–2153, Apr. 2016.
[23] J. Xu, L. Duan, and R. Zhang, "Cost-aware green cellular networks with energy and communication cooperation," *IEEE Commun. Mag.*, vol. 53, no. 5, pp. 257–263, May 2015.
[24] Q. Ye *et al.*, "User association for load balancing in heterogeneous cellular networks," *IEEE Trans. Wireless Commun.*, vol. 12, no. 6, pp. 2706–2716, Jun. 2013.
[25] K. Shen and W. Yu, "Distributed pricing-based user association for downlink heterogeneous cellular networks," *IEEE J. Sel. Areas Commun.*, vol. 32, no. 6, pp. 1100–1113, Jun. 2014.
[26] X. Fang, S. Misra, G. Xue, and D. Yang, "Smart grid—the new and improved power grid: A survey," *IEEE Commun. Surveys Tut.*, vol. 14, no. 4, pp. 944–980, 4th Quart. 2012.
[27] M. R. Garey and D. S. Johnson, *Computer and Intractability: A Guide to the Theory of NP-Completeness*. San Francisco, CA, USA: Freeman, 1979.
[28] A. J. Conejo, E. Castillo, R. García-Bertrand, and R. Mínguez, *Decomposition Techniques in Mathematical Programming: Engineering and Science Applications*. Berlin, Germany: Springer-Verlag, 2006.
[29] S. Boyd and J. Mattingley, "Branch and bound methods," Stanford Univ., Stanford, CA, USA, Lecture Notes for EE364b, pp. 2006–2007, 2007.
[30] S. Boyd and L. Vandenberghe, *Convex Optimization*. New York, NY, USA: Cambridge Univ. Press, 2004.
[31] Y.-F. Liu, Y.-H. Dai, and Z.-Q. Luo, "Joint power and admission control via linear programming deflation," *IEEE Trans. Signal Process.*, vol. 61, no. 6, pp. 1327–1338, Mar. 2013.
[32] R. D. Yates, "A framework for uplink power cellular radio systems," *IEEE J. Sel. Areas Commun.*, vol. 13, no. 7, pp. 1341–1347, Sep. 1995.
[33] G. J. Foschini and Z. Miljanic, "A simple distributed autonomous power control algorithm and its convergence," *IEEE Trans. Veh. Technol.*, vol. 42, no. 4, pp. 641–646, Nov. 1993.

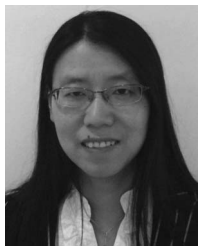

Min Sheng (M'03–SM'16) received the M.Eng. and Ph.D. degrees in communication and information systems from Xidian University, Xi'an, China, in 1997 and 2000, respectively.

She is currently a Full Professor with the Broadband Wireless Communications Laboratory, School of Telecommunication Engineering, Xidian University. She has published two books and over 50 papers in refereed journals and conference proceedings. Her general research interests include mobile ad hoc networks, wireless sensor networks, wireless mesh networks, third-generation/fourth-generation mobile communication systems, dynamic radio resource management for integrated services, cross-layer algorithm design and performance evaluation, cognitive radio and networks, cooperative communications, and medium access control protocols.

Dr. Sheng received the New Century Excellent Talents in University award from the Ministry of Education of China and received the Young Teachers Award from the Fok Ying-Tong Education Foundation, China, in 2008.

Daosen Zhai received the B.E. degree in telecommunication engineering from Shandong University, Weihai, China, in 2012. He is currently working toward the Ph.D. degree in communication and information systems with Xidian University, Xi'an, China.

His research interests focus on radio resource management in energy harvesting networks, topology control and connectivity analysis in ad hoc networks, and convex optimization and graph theory and their applications in wireless communications.

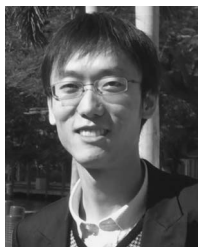

Xijun Wang (M'12) received the B.S. degree (with distinction) in telecommunications engineering from Xidian University, Xi'an, China, in 2005 and the Ph.D. degree in electronic engineering from Tsinghua University, Beijing, China, in 2012.

Since 2012, he has been with the School of Telecommunications Engineering, Xidian University, where he is currently an Associate Professor. His research interests include wireless communications, cognitive radios, and interference management.

Dr. Wang has served as a Publicity Chair for the 2013 IEEE/CIC International Conference on Communications in China (ICCC). He received the 2005 Outstanding Graduate of Shaanxi Province Award, the Excellent Paper Award at the 6th International Student Conference on Advanced Science and Technology in 2011, and the Best Paper Award at IEEE/CIC ICCC 2013.

Yuzhou Li received the B.Eng. degree in electronic and information engineering from Jilin University, Changchun, China, in 2009 and the Ph.D. degree in communication and information systems from Xidian University, Xi'an, China, in 2015.

He is currently an Assistant Professor with the Huazhong University of Science and Technology, Wuhan, China. His research interests include green communications, wireless resource allocation, and convex optimization and stochastic network optimization and their applications in wireless communications.

Authorized licensed use limited to: Huazhong University of Science and Technology. Downloaded on July 19,2024 at 08:11:44 UTC from IEEE Xplore. Restrictions apply.

Yan Shi (M'10) received the Ph.D. degree from Xidian University, Xi'an, China, in 2005.

He is currently an Associate Professor with the State Key Laboratory of Integrated Service Networks, Xidian University. His research interests include cognitive networks, modern switching technologies, and distributed wireless networking.

Jiandong Li (M'96–SM'05) received the B.E., M.S., and Ph.D. degrees in communications engineering from Xidian University, Xi'an, China, in 1982, 1985, and 1991, respectively.

Since 1985, he has been a faculty member with the School of Telecommunications Engineering, Xidian University, where he is currently a Professor and the Vice Director of the Academic Committee of the State Key Laboratory of Integrated Service Networks. From 2002 to 2003, he was a Visiting Professor with the Department of Electrical and Computer Engineering, Cornell University, Ithaca, NY, USA. His major research interests include wireless communication theory, cognitive radio, and signal processing.

Dr. Li served as the General Vice Chair for the 2009 International Conference on Communications and Networking in China and the Technical Program Committee Chair for the 2013 IEEE International Conference on Communications in China. He was awarded as a Distinguished Young Researcher by the National Natural Science Foundation of China and a Changjiang Scholar by the Ministry of Education, China.

Authorized licensed use limited to: Huazhong University of Science and Technology. Downloaded on July 19,2024 at 08:11:44 UTC from IEEE Xplore. Restrictions apply.